

EFFECTS OF PARTICLE-SIZE DISTRIBUTION AND STREAM GRADIENT ON SEDIMENT SORTING OF A DEBRIS FLOW

TAKASHI WADA

Department of Social Systems and Civil Engineering, Tottori University, Japan, wada-t@tottori-u.ac.jp

JUMPEI MAEDA

Department of Social Systems and Civil Engineering, Tottori University, Japan, m19j6028u@edu.tottori-u.ac.jp

HIROSHI MIWA

Department of Social Systems and Civil Engineering, Tottori University, Japan, miwa-h@tottori-u.ac.jp

ABSTRACT

We conducted flume experiments with sediment mixtures to reveal the effects of particle-size distribution and stream gradient on sediment sorting of a debris flow, focusing on the concentration of coarser particles that appeared at the flow front. In our experimental results, as the particle sizes of the sediment material became coarser or the flume gradient became lower, the sediment sorting progressed more remarkably. A possible reason for this is the decreasing of debris flow velocities, considering that the lowering of flume gradient and the enlargement of particle sizes of the materials decrease them. Since their changes influence the movement of materials in the depth direction, Middleton's suggested mechanism (1970), which is a falling mechanism of finer particles through the interstice between the materials in the flow's interior, may explain sediment sorting of a debris flow. In consideration of these results, we developed a numerical model to describe the sediment sorting based on the conventional one-dimensional model. In our model, the debris flow depth is divided into the several layers with the same thicknesses. The migration velocity of materials and the sediment concentration of each sized particle are considered in each divided layer. The volume of downward movement of each sized particle is also incorporated. The calculated results using our model indicate the concentration of coarser particles at the debris flow front. In addition, our model could explain temporal changes in the proportions of each sized particle of the flow on various particle-size distributions of the materials and various slope gradients.

Keywords: Debris flow, Concentration of coarser particles, Flow front, Stream gradient, Particle-size distribution

1. INTRODUCTION

Debris flows are composed of sediment particles of various sizes. Coarser particles become concentrated toward the flow front during down flow in mountainous streams. This phenomenon implies that sediment sorting occurs in the flow's interior during down flow. In particular, in a debris flow that includes many boulders, there is a tendency for the boulders to be concentrated toward the flow front, as reported in many field studies (e.g., Sharp et al., 1953; Okuda et al., 1977; Suwa et al., 1984; Suwa et al., 1986; Teramoto et al., 2002). Additionally, this phenomenon has been observed in many flume experiments related to a debris flow with sediment mixture (e.g., Hashimoto and Tsubaki, 1983; Miyamoto, 1986; Suwa, 1988; Takahashi et al., 1992; Satofuka et al., 2007; Iverson et al., 2010; Iwata et al., 2013). The devastation and loss of life caused by a debris flow on flooding areas such as alluvial fans can be extensive since the destructive force at the flow front becomes enlarged by this characteristic. To minimize or prevent these damages, it is necessary to accurately predict the concentration of coarser particles at the flow front arriving in the flooding areas. Therefore, a practical method is required to predict sediment sorting in the debris flow's interior, including the concentration of coarser particles at the flow front during down flow in mountainous streams.

Since the gradient of mountainous streams varies longitudinally, it is necessary to investigate the effects of stream gradient on sediment sorting in the debris flow's interior in order to accurately predict the concentration of coarser particles at the flow front arriving in the flooding areas. In addition, since the particle-size distributions of debris flows are various, it is also necessary to accurately investigate the effects of them on the sediment sorting. To gain insight into the effects of particle-size distribution and stream gradient on the sediment sorting, we conducted flume experiments with a tilted straight flume using sediment mixtures composed of particles of two different sizes. And then, we developed a numerical model to describe the changing particle-size distribution in the debris flow's interior and the concentration of coarser particles at the flow front based

on the model proposed by Satofuka et al. (2007). The validity of our model was examined by comparing the experimental results and the calculated results using our model.

2. FLUME EXPERIMENTS

2.1 Materials and methods

Figure 1 shows the experimental setup for the flume experiments, which consisted of a tilted straight flume with a length of 90 cm long and a width of 7 cm, and a movable sampler with four boxes. The sediment materials were composed of particles of two different sizes chosen from four sizes in the range of 1.4–10.7 mm; the mass density of the materials (σ) was 2.635 g/cm³, and the concentration in the static sediment bed (C_*) was 0.558. The ratios of coarser and finer particles in the materials were 1:1 or 1:4.

The experiments combined various conditions based on two key factors; the particle-size distribution of the materials and the flume gradient (stream gradient). Table 1 lists the experimental cases and their conditions. In these cases, the rate of supplied water was set to 67 cm²/s per a unit width.

The experimental procedure is described as follows. After the materials were set on the flume, water was supplied as the default flow rate at the upstream end of the flume. As the flow moved down the flume, the water eroded the materials and then a debris flow was generated. When the debris flow arrived at the downstream end of the flume, the flow encountered the sampler moving at a constant speed in the transverse direction with respect to the flow direction. The debris flow front was separated by the sampler into the four boxes over a constant time interval in the range of 1–2 seconds. Each time interval was measured by recording the material flowing into each box with a video. Measurements were performed to determine the temporal changes in the total flow discharge, sediment discharge, sediment flux concentration, and proportion of each sized particle in each sample. The above processes and measurements were repeated three times for each case, and for each flume gradient. In the analysis of our experimental results, we also used the previous experimental results for sediment sorting of a debris flow, which was composed of particles of two different sizes, reported by Miyamoto (1986). The sediment materials of the experiment were composed of particles of two different sizes chosen from five sizes in the range of 2–15 mm; the ratios of coarser and finer particles in the materials were 1:1 or 1:4. The inflow rate of water was set to 100–300 cm²/s per a unit width, the flow length was 1,200 cm, and the flume gradients were set to 15, 17, 20 and 22° in the experiment.

2.2 Experimental results

Figure 2 shows the temporal changes in the sediment flux concentrations of all sized particles and the proportion of each sized particle of the debris flows, obtained at the downstream end of the flumes in cases 1.2 [15°] and 4.1 [20°]. The proportions of coarser particles in the flow's interior increased more as being closer to the flow front, whereas the proportions of finer particles decreased. This tendency occurred in all cases and on all flume gradients. Therefore, the coarser particles became concentrated at the flow front during down flow regardless of the flume gradient or particle-size distribution of the material.

Figure 3 shows the proportion of each sized particle at the flow fronts at the downstream end of the flume in all cases; note that the flow front refers to the sediment material that flowed into the first box of the movable sampler at the downstream end, and the plots in the figure represent the mean value of the results of three runs in each case. In cases 1.1–6.1, with materials in which the ratios of coarser and finer particles were 1:1, the proportions of coarser particles at the flow front on the flume gradient of 20° were larger than those on 15° and

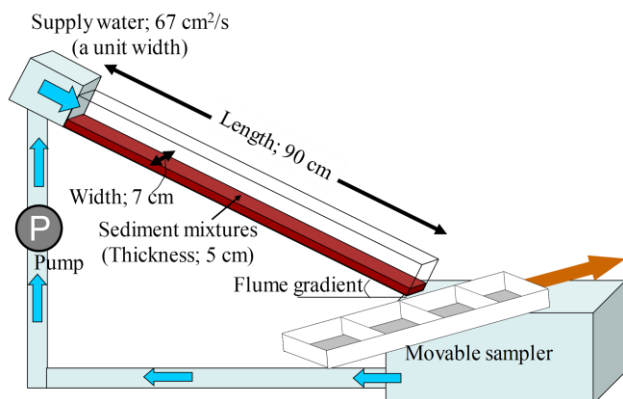


Figure 1. Experimental setup.

Table 1. Experimental cases and conditions.

Case	Particle-size distribution of material (Diameter; ratio)	Flume gradient (°)
Case 1.1	10.7 mm; 50%, 7.1 mm; 50%	15, 20, 25
Case 1.2	10.7 mm; 20%, 7.1 mm; 80%	
Case 2.1	10.7 mm; 50%, 3.0 mm; 50%	
Case 2.2	10.7 mm; 20%, 3.0 mm; 80%	15, 20, 25
Case 3.1	10.7 mm; 50%, 1.4 mm; 50%	
Case 3.2	10.7 mm; 20%, 1.4 mm; 80%	
Case 4.1	7.1 mm; 50%, 3.0 mm; 50%	15, 20, 25
Case 4.2	7.1 mm; 20%, 3.0 mm; 80%	
Case 5.1	7.1 mm; 50%, 1.4 mm; 50%	
Case 5.2	7.1 mm; 20%, 1.4 mm; 80%	15, 20, 25
Case 6.1	3.0 mm; 50%, 1.4 mm; 50%	
Case 6.2	3.0 mm; 20%, 1.4 mm; 80%	

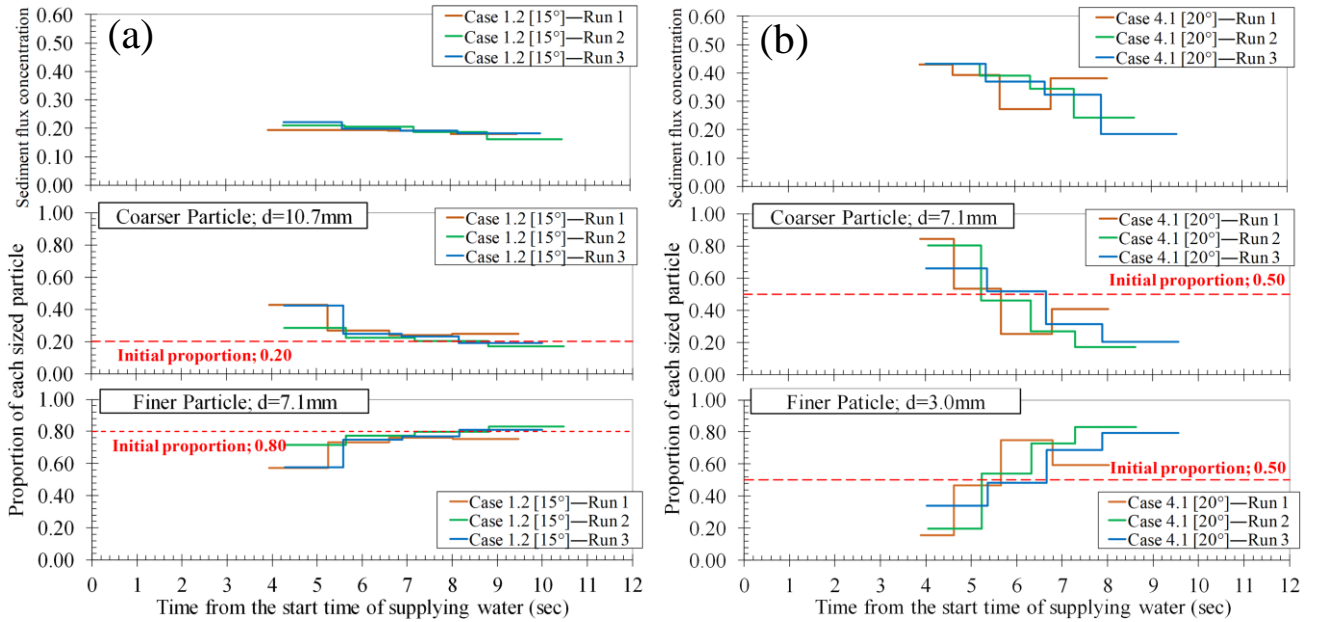


Figure 2. Temporal changes in sediment flux concentrations of all sized particles and proportion of each sized particle of the debris flows, obtained at the downstream end of the flumes; (a) Case 1.2 [15°], (b) Case 4.1 [20°].

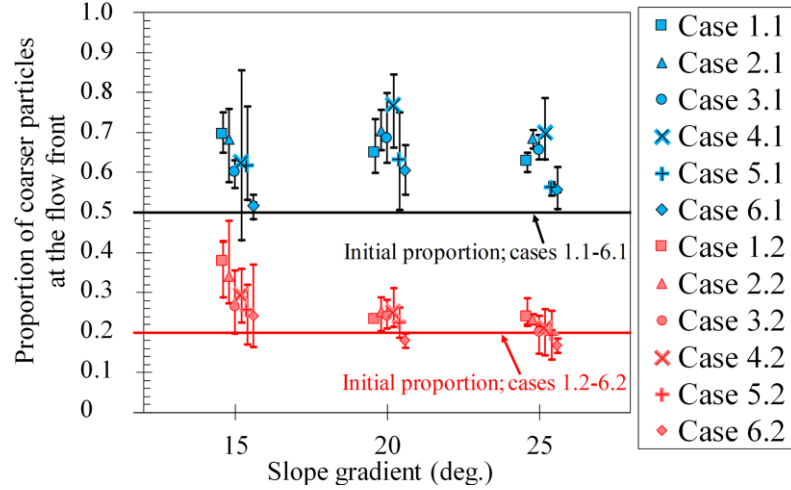


Figure 3. Proportion of each sized particle at the debris flow fronts, obtained at downstream end of the flume in all cases.

25°. Whereas, in cases 1.2–6.2, with materials in which the ratios of coarser and finer particles were 1:4, as the flume gradient lowered, the proportions of coarser particles at the flow front increased.

Figure 4 shows the relationship between the proportion of coarser particles at the flow front and the mean volume diameter of the material (d_m); note that the plots represent the mean value of the results of three runs in each case, and the previous results by Miyamoto (1986) were included in the figure. In both results, as the particle sizes of the material became coarser, the sediment sorting at the flow front progressed more remarkably. However, the proportions of coarser particles at the flow front in our results were smaller than that in the previous results by Miyamoto (1986). A possible reason for this was that the smaller inflow rate and the shorter flow length than his experiment were not enough to the progressing of the sediment sorting.

Figure 5 shows the relationship between the proportion of coarser particles at the flow front and the average velocity of the debris flow (U_m); note that the plots represent the mean value of results of three runs in each case and the previous results by Miyamoto (1986) were included in the figure. U_m was calculated with Eq. (1), that was obtained by integrating the theoretical equation for the velocity distribution of a steady uniform debris flow by Takahashi (1980).

$$U_m = \frac{2}{5d_m} \left[\frac{g \sin \theta}{\alpha_i \sin \phi} \left\{ C_d + (1 - C_d) \left(\frac{\rho_m}{\sigma} \right) \right\} \right]^{1/2} \left\{ \left(\frac{C_*}{C_d} \right)^{1/3} - 1 \right\} h^{3/2} \quad (1)$$

where g is the gravitational acceleration, θ is the flume gradient, ϕ is the internal friction angle of the material, α_i is the coefficient ($= 0.042$), C_d is the equilibrium sediment concentration ($= \rho_m \tan \theta / \{ (\sigma - \rho_m) (\tan \phi - \tan \theta) \}$), ρ_m is the mass density of interstitial fluid, and h is the flow depth. As shown in Figure 5, as U_m became larger, the proportions of coarser particles at the flow front increased in both results. In addition, in the cases of same flume gradient with different particle-size distribution, as U_m became smaller, the proportions of coarser particles at the flow front increased in both results.

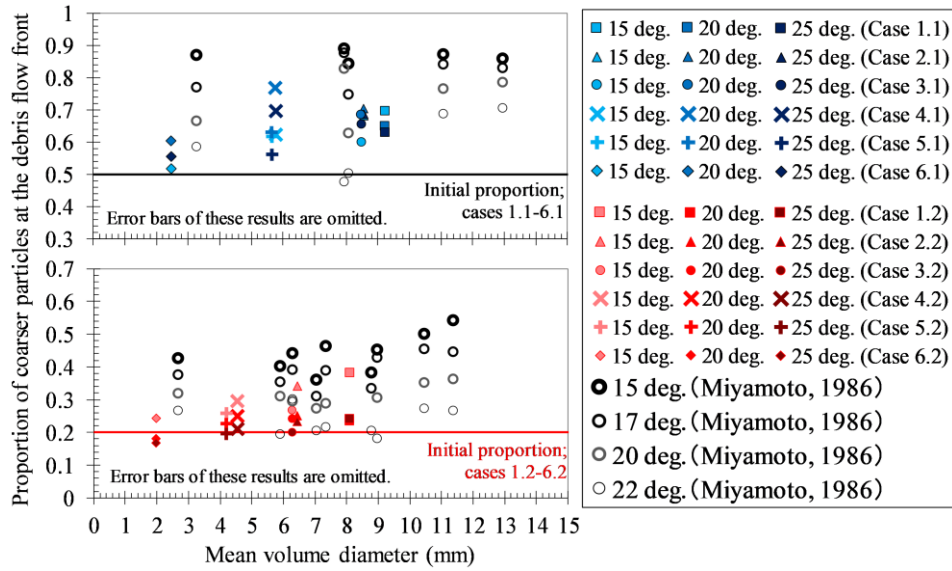


Figure 4. Relationship between proportions of coarser particles at debris flow front at downstream end of the flume and mean volume diameters of materials in all cases.

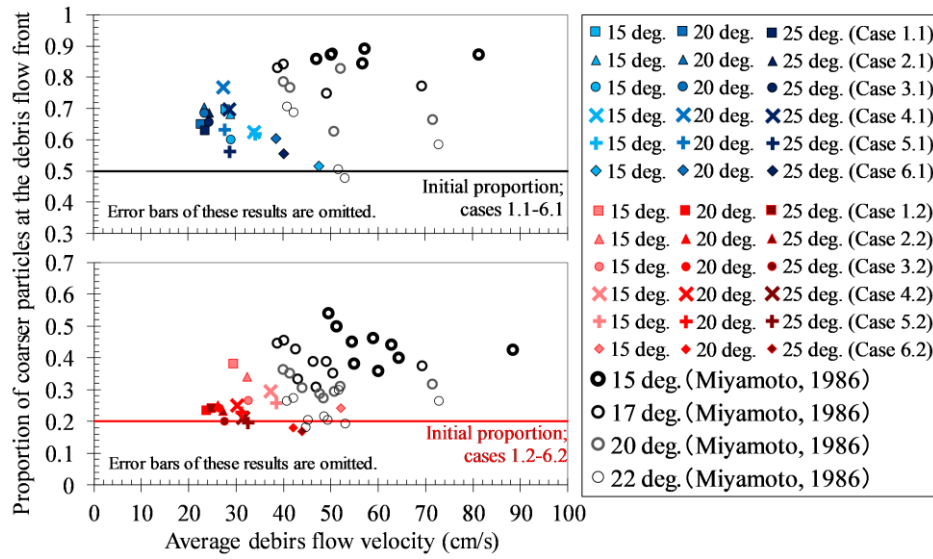


Figure 5. Relationship between proportions of coarser particles at debris flow front at downstream end of the flume and average velocities of debris flows in all cases.

2.3 Discussion about factors that influence the concentration of coarser particles at the debris flow front

According to the considerations in 2.2, as the particle sizes of the materials became coarser (this means that d_m became coarser) or the flume gradient ($\tan\theta$) became lower, the concentration of coarser particles at the flow front progressed more remarkably. Lowering the flume gradient and enlarging the particle sizes of the materials decrease the debris flow velocities, so that decreasing the debris flow velocities might be one of the reasons that caused the sediment sorting to progress more remarkably. Since varying the debris flow velocities may influence the movement of materials in the depth direction, Middleton's suggested mechanism (1970), which is a falling mechanism of finer particles through the interstice between the materials in the flow's interior (dynamic sieving), may explain this phenomenon. In the mechanism, the coarser particles which exist relatively in the upper layer of the flow's interior move by the faster velocities in the flow direction. That may be the reason why the proportions of coarser particles at the flow front were increasing more as U_m became larger.

3. APPLICATION WITH ONE-DIMENSIONAL NUMERICAL MODEL CONSIDERING SEDIMENT SORTING OF A DEBRIS FLOW

3.1 Outline of our developed model

We developed a numerical model to describe the changing particle-size distribution in the debris flow's interior and the concentration of coarser particles at the flow front based on the one-dimensional numerical model proposed by Satofuka et al. (2007).

Figure 6 shows an outline of our developed model. In our model, the debris flow depth (h) is divided into several layers with the same thicknesses, where n_p is the number of divided layers and D_L is the thickness of the divided layer ($= h / n_p$). Considering the theoretical equations for distributions of velocity and sediment concentration

Table 2. Calculation parameters.

Parameters/Variables	Value	Unit
Total simulation time	30	sec
Time step Δt	1.0×10^{-4}	sec
	10.70	
Diameters of particles d_k (two of four particle diameters)	7.10 3.00	mm
	1.40	
Mass density of material σ	2635	kg/m ³
Mass density of interstitial fluid ρ_m	1000	kg/m ³
Concentration in the static sediment bed C_*	0.558	–
Internal friction angle of material ϕ	32.85	deg.
Gravity acceleration g	9.8	m/s ²
Coefficient of erosion rate δ_e	0.03	–
Coefficient of accumulation rate δ_d	0.05	–
Interval of calculation points Δx	0.01	m
Coefficient to be related to the falling of particles α	5.0×10^2	–
Number of the divided layers n_p	4	–

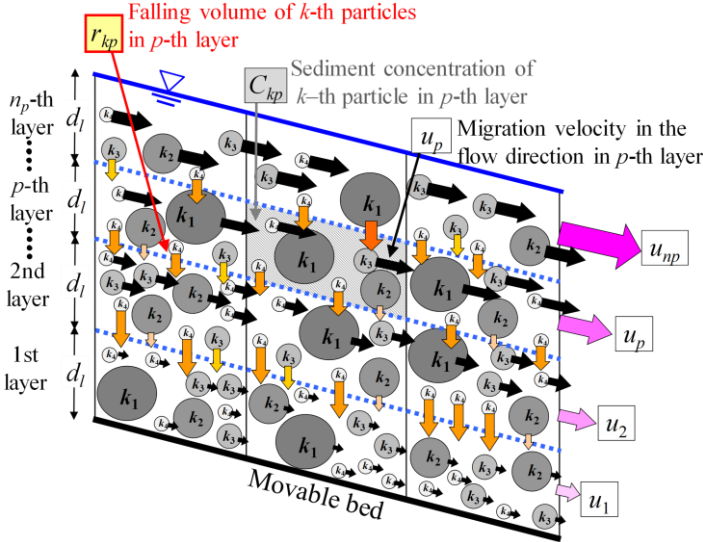


Figure 6. Outline of our developed 1-D model.

of a debris flow by Takahashi et al. (1996), the migration velocity of materials (u_p) and the sediment concentration of k -th particles (C_{kp}) are considered in each divided layer. The expression of C_{kp} is as follows:

$$C_{kp} = P_{kp} n_p \bar{C}_k \quad (2)$$

where P_{kp} is the proportion of k -th particles in the p -th layer and \bar{C}_k is the sediment concentration of k -th particles in the total flow layer as follows:

$$\bar{C}_k = \frac{C_{k1} + C_{k2} + C_{k3} + \dots + C_{kn_p}}{n_p} = \frac{\sum_{p=1}^{n_p} C_{kp}}{n_p} \quad (3)$$

In addition, the falling volume of k -th particles in the p -th layer (r_{kp}) is incorporated. Considering our experimental results (See 2.3), based on Middleton's suggested mechanism (dynamic sieving), we consider r_{kp} is proportional to the cube of s_{p-1}/d_k and proportional to $\Delta u/\Delta z$ expediently. The expression of r_{kp} is as follows:

$$r_{kp} = \alpha \left(\frac{s_{p-1}}{d_k} \right)^3 \frac{\Delta u}{\Delta z} C_{kp} D_L = \alpha \left[\frac{dm_{p-1}}{d_k} \left\{ \left(\frac{\sum_{k=1}^{k_e} C_{k,p-1}}{C_*} \right)^{1/3} - 1 \right\} \right]^3 \frac{\Delta u}{\Delta z} C_{kp} D_L \quad (4)$$

where α is the coefficient related to the falling of particles, s_p is the interstice between particles in the p -th layer, which is evaluated on the equidistant particle arrangement of the flow including highly-concentrated particles proposed by Bagnold (1954), d_k is the diameter of k -th particles, dm_p is the mean volume diameter of all particles in the p -th layer, k_e is the number of particle classes, and $\Delta u/\Delta z$ is the velocity gradient (shear strain) between the p -th and $p-1$ th layers.

3.2 Governing equations

The governing equations of our developed model are briefly discussed as follows. The momentum equation for the flow mixture in the total flow layer, the continuity equation for the flow mixture in the total flow layer, the continuity equation of k -th particles in the p -th layer, and the equation of bed variation are given as Eqs. (5), (6), (7) and (8), respectively:

$$\frac{\partial M}{\partial t} + \beta \frac{\partial uM}{\partial x} = -gh \frac{\partial(z_b + h)}{\partial x} - \frac{\tau_b}{\rho_m} \quad (5)$$

$$\frac{\partial h}{\partial t} + \frac{\partial M}{\partial x} = \sum_{k=1}^{k_e} i_{bk} \quad (6)$$

$$\frac{\partial C_{kp} D_L}{\partial t} + \frac{\partial q_{bkp}}{\partial x} = \frac{\partial P_{kp} \bar{C}_k h}{\partial t} + \frac{\partial u_p P_{kp} \bar{C}_k h}{\partial x} = \begin{cases} i_{bk} C_* - r_{k2} - r'_{k1} & (p = 1) \\ (r_{kp} - r_{k,p+1}) - (r'_{kp} - r'_{k,p-1}) & (1 < p < n_p) \\ r_{kn_p} + r'_{k,n_p-1} & (p = n_p) \end{cases} \quad (7)$$

$$\frac{\partial z_b}{\partial t} + \sum_{k=1}^{k_e} i_{bk} = 0 \quad (8)$$

where t is the time, x is the coordinate axis of the flow direction, β is the momentum coefficient ($= 1$), M is the momentum flux for the total flow layer ($=uh$), z_b is the height of the movable bed, τ_b is the shear resistance of the river bed, i_{bk} is the sediment erosion/deposition velocity of k -th particles, q_{bkp} is the transportation volume of k -th particles per a unit width in the flow direction in the p -th layers ($=u_p C_{kp} h/n_p$), and r_{kp} is the transportation volume of k -th particles from the p -1th layer to the p -th layer, which is the surplus volume for the maximum volume in the p -1th layer obtained by the theoretical equation for distributions of sediment concentration by Takahashi et al. (1996). τ_b , i_{bk} and temporal changes in particle-size distribution of the movable bed are the same as those used by Nakagawa et al. (1996); for a more detailed explanation, please refer to the original report.

3.3 Calculation result

We performed calculations to reproduce our experiments by using our developed model. Table 2 lists the parameters used in the calculations.

Figure 7 shows the calculated longitudinal results of the debris flow height, the mean volume diameter in the flow's interior, the sediment concentration and the proportion of each sized particle in each layer 3.5 seconds after supplying water at the upstream end of the flume in cases 1.2 [15°] and 4.1 [20°]. The calculated results by using our model indicate the proportion of coarser particles increase as being closer to the flow front and upper in the flow's interior. Therefore, our model can explain that the coarser particles exist relatively in the upper layer of the flow's interior and concentrate at the flow front during downflow.

Figure 8 shows the comparison between the experimental results and calculated results for the temporal changes in the proportion of each sized particle of the debris flows, obtained at the downstream end of the flume in cases 1.2 [15°] and 4.1 [20°]. In the calculated results, the proportions of coarser particles are the most at the flow front and decrease as being far from the front. Whereas, the proportions of finer particles are the least at the

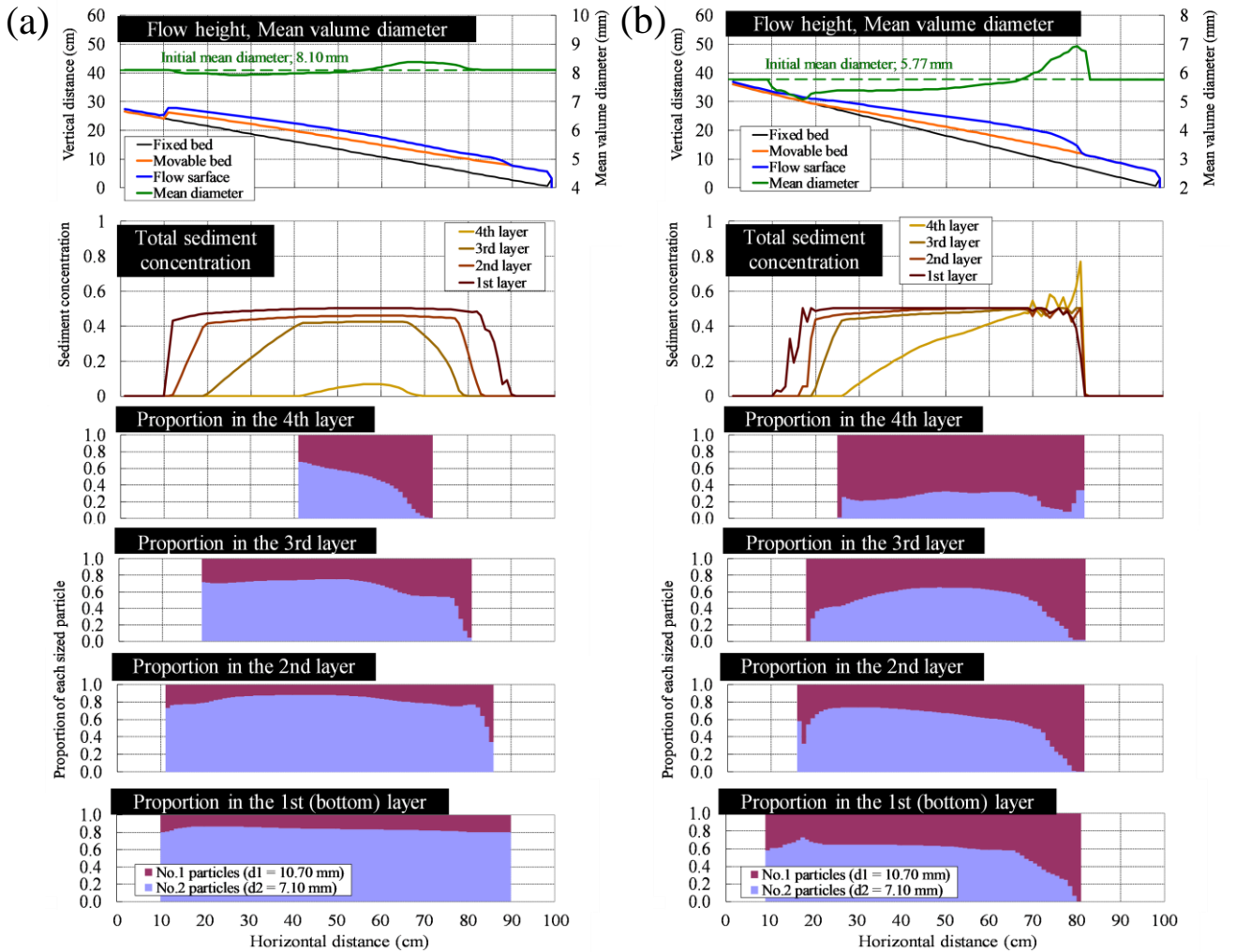


Figure 7. Calculated longitudinal results of debris flow height, mean volume diameter in debris flow's interior, sediment concentration and proportion of each sized particle in each layer 3.5 seconds after supplying water at upstream end of the flumes; (a) Case 1.2 [15°], (b) Case 4.1 [20°].

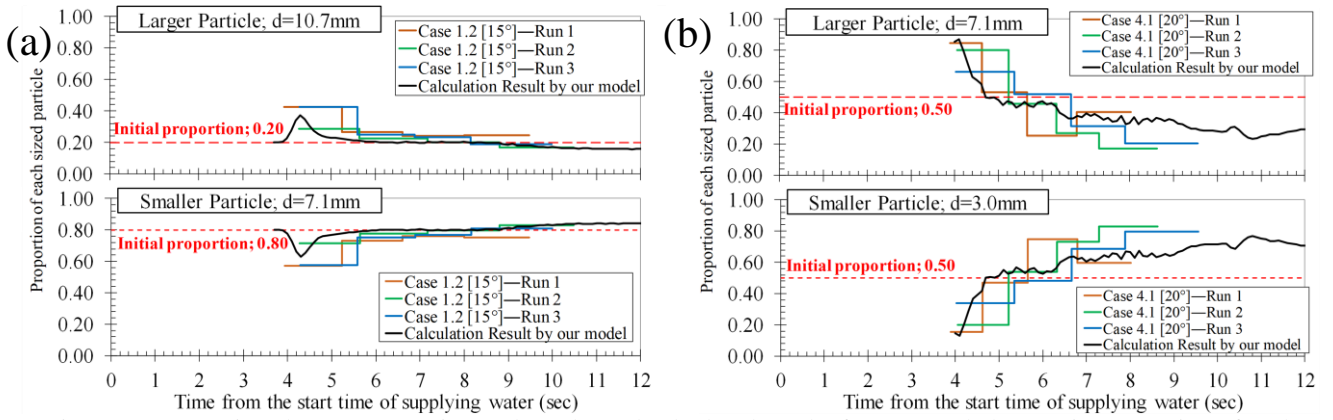


Figure 8. Comparison between experimental results and calculated results for temporal changes in proportion of each sized particle of the debris flows at downstream end of the flume; (a) Case 1.2 [15°], (b) Case 4.1 [20°].

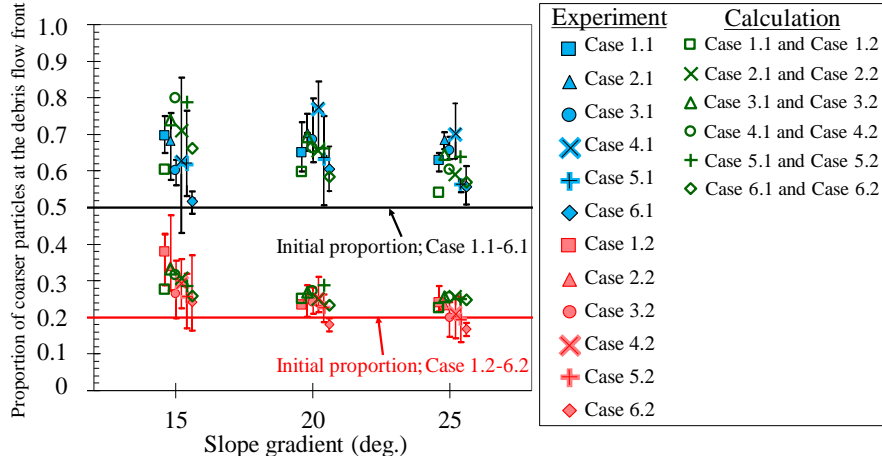


Figure 9. Comparison between experimental results and calculated results for proportions of coarser particles at debris flow front at downstream end of the flume.

flow front and increase as being far from the front. These tendencies are quantitatively consistent with the experimental results.

Figure 9 shows the comparison between the experimental results and calculated results for the proportions of coarser particles at the flow front, obtained at the downstream end of the flume in all cases. In the calculation results, the debris flow front is defined to the range of 1–2 seconds after passing of the flows at the downstream end, which is the same range of flowed into the first box of the movable sampler in our experiments. The calculated results are almost consistent with the experimental results in all cases. However, in the case that the sizes of coarser and finer particles are relatively large and similar (e.g. cases 1.1), the calculated results underestimate the experimental results. The reason for these results is that describing sediment sorting of a debris flow in our model depends only on the Middleton's mechanism, that is falling of finer particles into the interstice between particles. Therefore, in order to describe this more accurately, incorporating the rising of coarser particles caused by a collision or contact between particles in the flow's interior is required in our model. In addition, in the almost cases with materials in which the ratios of coarser and finer particles are 1:1 and the flume gradients are 15°, the calculated results overestimate the experimental results. In these cases, the debris flows have the lower capacity for sediment transport by the shorter flow distance and the lower flume gradient relatively. Considering the above, transporting the sediment to the flow fronts and concentrating of coarser particles at the flow fronts can be insufficient when the flows arrive at the downstream end. Therefore, the reason for the inconsistency with the experimental results and calculated results in these cases is that overestimating of sediment transport of the debris flows in our model. Thus, enhancing the accuracy of sediment transport in the flow's interior is also required in our model.

4. CONCLUSIONS

In this study, we conducted flume experiments with sediment mixtures to reveal the effects of particle-size distribution and stream gradient on sediment sorting of a debris flow, focusing on the concentration of coarser particles that appeared at the flow front. As the particle sizes of the materials became coarser or the flume gradient became lower, the sediment sorting at the flow front progressed more remarkably. Since lowering the flume gradient and enlarging the particle sizes of the materials decrease the debris flow velocities, decreasing the debris flow velocities might have caused the sediment sorting to progress more remarkably. In addition,

since decreasing the debris flow velocities enlarges the movement of materials in the depth direction, Middleton's suggested mechanism (1970) may explain sediment sorting of the flow.

Considering the above, we developed a numerical model to describe the changing particle-size distribution in the debris flow's interior and the concentration of coarser particles at the flow front based on the one-dimensional numerical model proposed by Satofuka et al. (2007). In our model, the debris flow depth is divided into several layers with the same thicknesses. Based on the theoretical equations for distributions of velocity and sediment concentration of a debris flow by Takahashi et al. (1996), the migration velocity of materials (u_p) and the sediment concentration of k -th particles (C_{kp}) are considered in each divided layer. Additionally, the falling volume of downward movement of k -th particles (r_{kp}) is incorporated.

Our model can explain that the coarser particles exist relatively in the upper layer of the flow's interior and concentrate at the flow front during downflow. In addition, our model can quantitatively explain temporal changes in the proportions of each sized particle of the flow on various particle-size distributions of the materials and various slope gradients. However, in some cases, the calculation results are inconsistent with the experimental results for the proportion of coarser particles at the flow front. The reason for these results is that describing sediment sorting of a debris flow in our model depends only on the Middleton's mechanism. Another reason for these results is the overestimating of sediment transport of the flow in our model. Therefore, in order to describe this more accurately, incorporating the rising of coarser particles caused by a collision or contact between particles and enhancing the accuracy of sediment transport in the debris flow's interior are required in our model. Furthermore, since our model is only based on the findings of several experiments under limited conditions, it is also necessary to evaluate the verification of our model quantitatively by using further experimental results.

REFERENCES

- Bagnold, R. A. (1954). Experiments on a gravity-free dispersion of large solid spheres in a Newtonian fluid under shear, *Proceedings of the Royal Society of London*, 225A:49–63.
- Hashimoto, H. and Tsubaki, T. (1983). Reverse grading in debris flow, *Journal of the Japan Society of Civil Engineers*, 336:75–84 (in Japanese).
- Iverson, R. M., Logan, M., LaHusen, R. G. and Berti, M. (2010). The perfect debris flow? Aggregated results from 28 large-scale experiments, *Journal of Geophysical Research*, 115:F03005.
- Iwata, T., Hotta, N. and Suzuki, T. (2013). Influence of particle-size segregation in multi-granular debris flow on the fluidity, *Journal of the Japan Society of Erosion Control Engineering*, 66,(3):13–23 (in Japanese with English abstract).
- Middleton, G. V. (1970). Experimental studies related to problems of flysch sedimentation, *Lajoie, J. ed., Flysch Sedimentology in North America, Geological Association of Canada Special Paper 7*, 253–272.
- Miyamoto, K. (1986). Mechanics of grain flows in Newtonian fluid, *Ph.D. Thesis Ritsumeikan Univ.*, 73–99 (in Japanese).
- Nakagawa, H., Takahashi, T., Sawada, T. and Satofuka, Y. (1996). Design hydrograph and evacuation planning for debris flow, *Annals of Disaster Prevention Research Institute, Kyoto Univ.*, 39(B-2):347–371 (in Japanese with English abstract).
- Okuda, S., Suwa, H., Okunishi, K., Nakano, M. and Yokoyama, K. (1977). Synthetic observation on debris flow part. 3 observation at valley Kamikamihorisawa of Mt. Yakedake in 1976, *Annals of Disaster Prevention Research Institute, Kyoto Univ.*, 20(B-1):237–263 (in Japanese with English abstract).
- Satofuka, Y., Iio, T. and Mizuyama, T. (2007). Sediment sorting in stony debris flow, *Proceedings of 4th International Conference on Debris-Flow Hazards Mitigation*.
- Sharp, R. P. and Nobles, L. H. (1953). Mudflow of 1941 at Wrightwood, southern California, *Bulletin of the Geological Society of America*, 64:547–560.
- Suwa, H. (1988). Focusing mechanism of large boulders to a debris-flow front, *Annals of Disaster Prevention Research Institute, Kyoto Univ.*, 31(B-1):139–151 (in Japanese with English abstract).
- Suwa, H. and Okuda, S. (1986). Size segregation of solid particles in debris flows (part.2) –size segregation in the debris flow on July, 1985 and experiment of size segregation by shearing a particle mixture–, *Annals of Disaster Prevention Research Institute, Kyoto Univ.*, 29(B-1):391–408 (in Japanese with English abstract).
- Suwa, H., Okuda, S. and Ogawa, K. (1984). Size segregation of solid particles in debris flows, part.1 –accumulation of large boulders at the flow front and inverse grading by kinetic sieving effect–, *Annals of Disaster Prevention Research Institute, Kyoto Univ.*, 27(B-1):409–423 (in Japanese with English abstract).
- Takahashi, T. (1980). Debris flow on prismatic open channel, *Journal of the Hydraulics Division, Proceedings of the American Society of Civil Engineer*, .106(HY3):381–396.
- Takahashi, T., Nakagawa, H., Harada, T. and Yamashiki, Y. (1992). Routing debris flows with particle segregation, *Journal of Hydraulic Engineering*, 118:1490–1570.
- Takahashi, T., Satofuka, Y., and Chishiro, K. (1996). Dynamical law of debris flows in inertial regime, *Annals of Disaster Prevention Research Institute, Kyoto Univ.*, 39(B-2):333–346 (in Japanese with English abstract).
- Teramoto, Y., Jitousono, T. and Shimoyama, E. (2002). Flow properties of the debris flow that occurred on September 11, 1999, in the Akamatsu-dani River Basin at Unzen Volcano, *Research Bulletin of Kagoshima Univ. Forest*, 30:19–25 (in Japanese with English abstract).